T-Wave Peak-to-End Morphology Restitution as Biomarker in Brugada Syndrome

Neurys Gómez[1,2], Julia Ramírez[1,2,3], Alba Isabel Roquero[4], Favio Palmieri[5], Elena Arbelo[4], Juan Pablo Martínez[1,2], Pablo Laguna[1,2]

[1] BSICoS Group, I3A, IIS Aragon, University of Zaragoza, Zaragoza
[2] Centro de Investigación Biomédica en Red – BBN (CIBER-BBN), Zaragoza, Spain
[3] William Harvey Research Institute, Queen Mary University of London, London, United Kingdom
[4] Faculty of Medicine and Health Sciences, University of Barcelona, Barcelona, Spain
[5] Arrhythmia Section, Cardiology Service, Hospital Clínic, Barcelona, Spain

Abstract

*Brugada syndrome (BrS) is a genetic disorder that affects the ion channels of the cardiac myocites, resulting in a higher predisposition to malignant ventricular arrhythmias and sudden cardiac death (SCD). Risk stratification and management of BrS patients remains a major clinical challenge. In this work, we use a time-warping-based index of the T-wave peak-to-end morphological restitution (*TPEMR*) to quantify the restitution properties of the late phase of ventricular repolarization and evaluate its ability to distinguish between control and BrS patients and between symptomatic (BrS-S) and asymptomatic patients (BrS-A). 24-hour Holter ECG recordings from 89 BrS patients (29 asymptomatic, BrS-A, and 60 symptomatic, BrS-S) and 32 healthy control patients were analyzed. The original, unweighted* $\text{TPEMR}_{\mathcal{O}}$ *as well as weighted versions with two different strategies* $\text{TPEMR}_{\mathcal{W}1}$ *and* $\text{TPEMR}_{\mathcal{W}2}$ *are computed.* TPEMR *derives from a time-warping,* $d^{\text{PCA}}_{w,\text{T}_{pe}}$*, index computed from T waves at two distant RR bins normalized by the RR range. All the three TPEMR indices were significantly higher for BrS group than for the control group. BrS-S group presented higher* TPEMR *indexes than BrS-A group for all indices, though significant differences were only shown in the weighted* $\text{TPEMR}_{\mathcal{W}2}$ *index.*

1. Introduction

Brugada syndrome (BrS) is a genetic disorder that affects the ion channels of the cardiac myocites, resulting in distinctive abnormal electrocardiographic patterns and a high predisposition to malignant ventricular arrhythmias and sudden cardiac death (SCD) [1]. Risk stratification and management of patients with BrS remains a major clinical challenge due to the lack of a single, accepted biomarker of SCD risk. To date, recovered SCD (RSCD) or arrhythmogenic syncope are considered the most robust risk indicators in these patients [2, 3].

Repolarization disorders is one of leading hypotheses regarding the pathophysiological mechanisms behind the Brugada pattern [4], which remain controversial. Heterogeneity in ventricular restitution properties has been linked to the development of repolarization dispersion gradients, which, when pronounced, increase the risk of malignant ventricular arrhythmias [5], so its evaluation in the context of patients with BrS seems relevant. However, directly action potential duration restitution dynamics (APDR) evaluation remains impractical due to its invasive nature, driving the development of indirect non-invasive alternatives. A T-wave morphology-based APDR index quantifying the variations in the overall morphology of the T-wave with heart rate, T-wave morphology restitution index (TMR) [6], has recently been reported and linked with SCD in chronic heart failure and general population.

This warping-based morphological index attempts to overcome the restrictions of time-interval-based indices that do not capture all possible morphological changes contained in the ECG waves. However, in the presence of typical Brugada patterns, the presence of coved ST segment elevation (type 1 Brugada pattern) or ssaddle-back ST elevation (type 2 Burgada pattern), largely distorting the T wave initial part, may advise against the use of TMR index. In addition, previous studies have shown that the dispersion of ventricular repolarization reflected in the T-peak-to-end (T_{pe}) interval, when captured by a warping-based index computed in a spatially transformed PCA lead, $d^{\text{PCA}}_{w,\text{T}_{pe}}$, has also potential for arrhythmia risk prediction [7], avoiding the earlier part of the T wave. These results suggest the exploration of this technique for risk stratification in BrS patients.

The present study aims to evaluate the TMR index,

adapted to specifically quantify variations in the $\mathrm{T_{pe}}$ morphology with heart rate, TPEMR, testing whether it can discriminate between control and BrS patients and between symptomatic (BrS-S) and asymptomatic (BrS-A) BrS patients.

2. Materials and Methods

2.1. Study Population

The study population included 89 patients with BrS (median[range] age: 53 [24; 81] years, 66.12% male, 33.06% type-I BrS) and 32 healthy control patients (median age: 25 [19; 70] years, 42.55% male). Of the total BrS population, 29 patients who experienced cardiac-related syncope and/or SCD events before ECG recording, as well those who suffered major events during follow up, were classified as symptomatic BrS patients group (BrS-S), while patients with no events were labeled as asymptomatic BrS patients group (BrS-A). ECG recordings were collected using a continuous 12-lead ECG Holter monitor (Spiderview Plus, Livanova-Sorin Group, ELA Medical, Montrouge, France) with a 2.5 μV amplitude resolution (16-bit) and a sampling frequency of 1000 Hz. High-positioned precordial leads, commonly used in BrS, were used in the recordings. This study was approved by the ethical committee of the Hospital Clínic of Barcelona (Reg. HCB/2020/0306) in accordance with ethical standards and deontological guidelines.

2.2. ECG Pre-Processing

ECG pre-processing included low-pass filtering (cut-off frequency of 40 Hz) to remove electrical and muscle noise and high-pass filtering (cut-off frequency of 0.5 Hz) to reduce baseline wander. In both cases, forward/backward sixth-order Butterworth filters were used. A wavelet-based single-lead ECG delineator [8] followed by a multilead delineation selection rule was applied. Next, spatial Principal Component Analysis (PCA) was applied to the 6 chest leads, learning the transformation coefficients from the correlations in the T wave segment to emphasize this wave. Finally, the first principal component transformed lead was delineated, each T-wave segmented and further low-pass filtered (20 Hz cut-off) for subsequent analysis.

2.3. Quantification of the T_{pe} Morphology Restitution

T-wave peak-to-end morphology restitution index, TPEMR, was measured for each patient using the method described in [9] for the time-warping quantification index, $d^{\mathrm{PCA}}_{w,\mathrm{T}_{pe}}$, and normalizing by the intrasubject RR range used for $d^{\mathrm{PCA}}_{w,\mathrm{T}_{pe}}$ derivation. Initially, the beats are clustered in bins based on their RR interval, and a histogram with 10-ms bins was generated with data from the entire 24-hour recording. Bins containing fewer than 15 beats were excluded from further analysis. Subsequently, the two more extreme RR intervals bins containing at least 500 beats were considered. From those bins, the one closer to the median bin was selected together with its symmetric bin with respect to the median, labeled as RR_1 and RR_2, were selected.

A mean warped T wave peak-to-end (MWTPE) was computed for each of the two selected bins, and $d^{\mathrm{PCA}}_{w,\mathrm{T}_{pe}}$ was computed as the temporal reparametrization between both MWTPE: $\boldsymbol{f^s}(\boldsymbol{t^s}) = [\boldsymbol{f^s}(\boldsymbol{t^s}(\mathbf{1})), ..., \boldsymbol{f^s}(\boldsymbol{t^s}(\boldsymbol{N_s}))]^{\boldsymbol{T}}$ from bin RR_1, where $\boldsymbol{t^s} = [t^s(1), ..., t^s(N_s)]^T$, and the analogously defined $\boldsymbol{f^r}(\boldsymbol{t^r})$ from bin RR_2 (see Fig 1b). Biphasic T-waves were discarded for the MWTPE estimation. If positive and negative T waves were present in the same bin, only the dominant class within that bin was considered to compute the MWTPE. The amount of warping needed to eliminate the time differences between them is quantified by the warping-based index $d^{\mathrm{PCA}}_{w,\mathrm{T}_{pe}}$ between these two MWTPEs, reflecting the variations on repolarization dispersion between T waves belonging to RR_1 and RR_2 bins.

The $d^{\mathrm{PCA}}_{w,\mathrm{T}_{pe}}$ index (the sum of the green and yellow areas in Fig 1c) measures the amount of warping needed to fit the two MWTPE waves [9].

The TPEMR index was calculated by dividing the absolute value of $d^{\mathrm{PCA}}_{w,\mathrm{T}_{pe}}$ by the RR range:

$$\mathrm{TPEMR} = \frac{|d^{\mathrm{PCA}}_{w,\mathrm{T}_{pe}}|}{\Delta\mathrm{RR}}. \quad (1)$$

where $\Delta\mathrm{RR} = \mathrm{RR}_2 - \mathrm{RR}_1$ (Fig 1a).

In order to attenuate the undesired effects of T wave delineation errors, we also estimated TPEMR based on two different versions of weighted warping-based $\mathrm{T_{pe}}$ index [10]. The weighted warping functions were proportional to the absolute value of the $\mathrm{T_{pe}}$ derivative ($\mathcal{W}1$) or to the absolute value of the $\mathrm{T_{pe}}$ amplitude ($\mathcal{W}2$) [10], this one represented in the yellow area in Fig. 1c. The different versions of TPEMR are denoted as $\mathrm{TPEMR}_{\mathcal{I}}$, with $\mathcal{I} \in \{\mathcal{O}, \mathcal{W}1, \mathcal{W}2\}$ denoting the original unweighted estimate ($\mathcal{O}$) or the weighted versions, respectively. The Kruskal-Wallis test was used for group comparisons. p-value$\leq$0.05 denotes statistical significance.

3. Results and Discussion

No significant differences were found in the shape variation of the T wave peak-to-end, quantified by $d^{\mathrm{PCA}}_{w,\mathrm{T}_{pe}}(\mathcal{O})$, between the control and BrS groups (2.45 [2.70] vs 3.80 [4.40] p-value = 0.1). The weighted versions $d^{\mathrm{PCA}}_{w,\mathrm{T}_{pe}}(\mathcal{W}1)$ or $d^{\mathrm{PCA}}_{w,\mathrm{T}_{pe}}(\mathcal{W}2)$ were not either significantly different when comparing between BrS and control groups with p-value

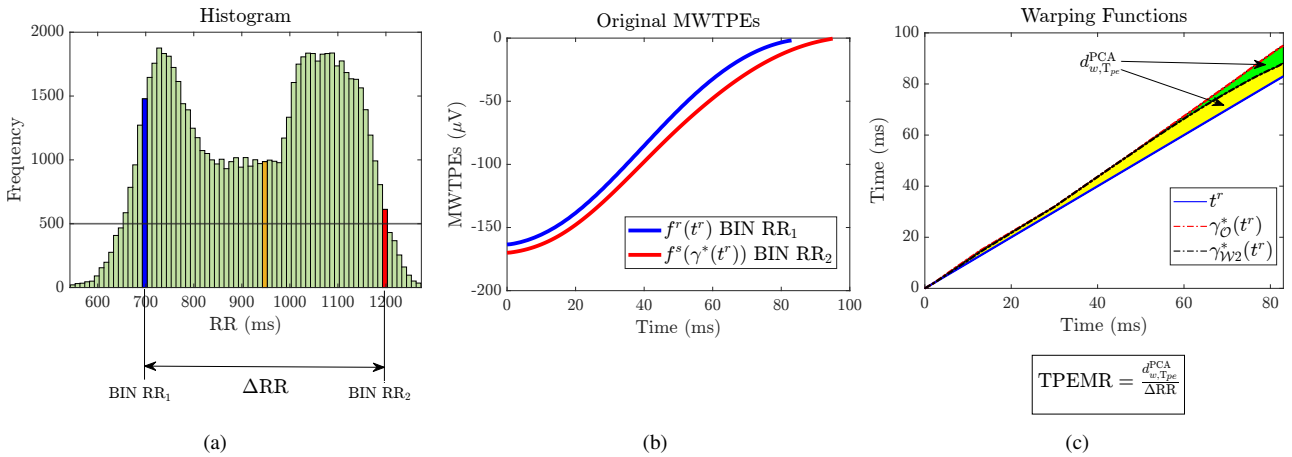

Figure 1: Estimation of the T-wave peak-to-end morphology restitution index, TPEMR. (a) Histogram of RR intervals; the orange bar indicates the median RR interval, while blue and red bars denote the two bins defining the maximum intra-subject RR range, ΔRR. (b) MWTPEs corresponding to the RR values highlighted in panel (a). (c) Estimation of the $d^{PCA}_{w,T_{pe}}$ index obtained by time-warping the two MWTPEs. The TPEMR index is calculated as $|d^{PCA}_{w,T_{pe}}|$ normalized by ΔRR.

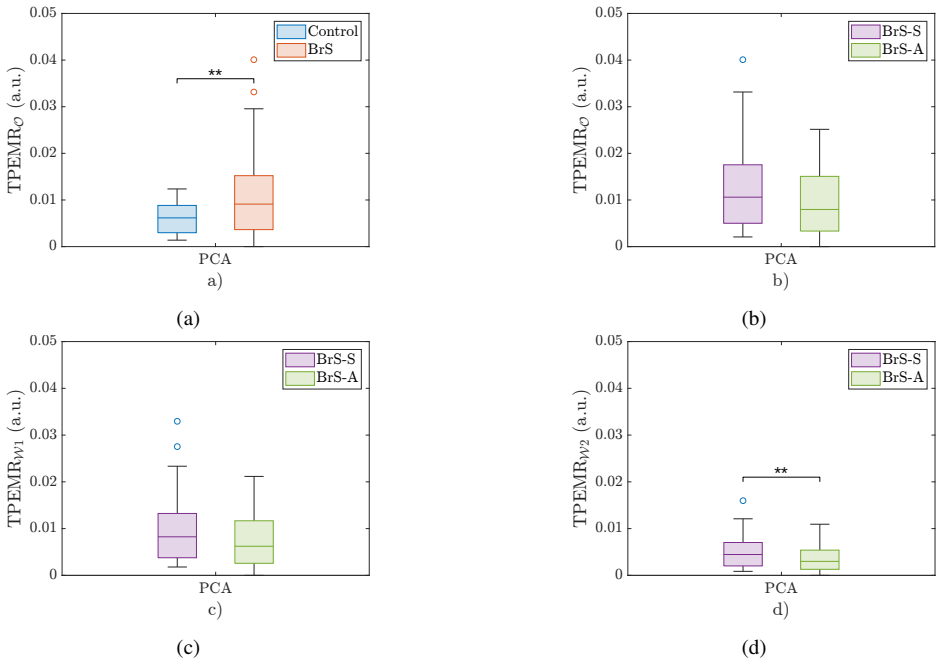

Figure 2: Box plots distributions of $TPEMR_{\mathcal{O}}$ index (a) for control (blue) and BrS (red) groups and for $TPEMR_{\mathcal{O}}$ (b), $TPEMR_{\mathcal{W}1}$ (c) and $TPEMR_{\mathcal{W}2}$ (d) indices for BrS-S (purple) and BrS-A (green) groups. ** indicates statistical significance.

of 0.068 and 0.063 respectively. Although non-significant, larger warping values in the BrS may indicate a trend towards a higher degree of ventricular repolarization dispersion in these patients. The median [IQR] and p-values for each index and patient group are shown in Table 1.

When comparing BrS-S and BrS-A groups, significant differences were found only for $d^{PCA}_{w,T_{pe}}(\mathcal{W}2)$ (1.94 [2.14] for BrS-S group vs 1.24 [1.40] for BrS-A group, $p = 0.027$). The other indices showed larger and more disperse values for the BrS-S group, but without reaching statistical significance. See more details in Table 1. These results point out that BrS-S patients have higher ventricular repolarization dispersion than BrS-A, as quantified by $d^{PCA}_{w,T_{pe}}(\mathcal{W}2)$, associated with the known higher risk of arrhythmias and SCD in BrS-S patients.

When analyzing ventricular repolarization restitution dynamics quantified by $TPEMR_{\mathcal{O}}$, $TPEMR_{\mathcal{W}1}$ and $TPEMR_{\mathcal{W}2}$, these indices better discriminated between

Table 1: Median[IQR] and p-value of $d^{\text{PCA}}_{w,\text{T}_{pe}}(\mathcal{O})$, $d^{\text{PCA}}_{w,\text{T}_{pe}}(\mathcal{W}1)$ and $d^{\text{PCA}}_{w,\text{T}_{pe}}(\mathcal{W}2)$ indices.

Group	$d^{\text{PCA}}_{w,\text{T}_{pe}}(\mathcal{O})$	$d^{\text{PCA}}_{w,\text{T}_{pe}}(\mathcal{W}1)$	$d^{\text{PCA}}_{w,\text{T}_{pe}}(\mathcal{W}2)$
CG	2.45 [2.70]	1.90 [2.13]	0.92 [0.94]
BrS	3.80 [4.40]	2.98 [3.47]	1.37 [1.50]
p-value	0.095	0.068	0.063
BrS-S	4.31 [6.24]	3.30 [4.54]	1.94 [2.14]
BrS-A	3.51 [3.76]	2.77 [3.08]	1.24 [1.40]
p-value	0.141	0.141	0.027

control and BrS groups. The three indices were significantly higher for the BrS group than for the control group (see Table 2). This suggests that Brugada syndrome is associated to higher restitution values of the late phase of ventricular repolarization, related to an increased transmural dispersion. In contrast with raw $d^{\text{PCA}}_{w,\text{T}_{pe}}$ indices which, by themselves, were not statistically different when comparing BrS and control groups, BrS patients presented significantly greater morphological changes in the T_{pe} interval per heart rate increase than control patients. As for the differences between symptomatic and asymptomatic patients, BrS-S group presented higher restitution values than BrS-A group with all three indices, but only with $\text{TPEMR}_{\mathcal{W}2}$ this difference was statistically significant, pointing to a higher arrhythmic risk for the symptomatic patients that needs to be further investigated. Figure 2 shows the box plots of the distributions of $\text{TPEMR}_{\mathcal{O}}$ for control and BrS groups and those of $\text{TPEMR}_{\mathcal{O}}$, $\text{TPEMR}_{\mathcal{W}1}$ and $\text{TPEMR}_{\mathcal{W}2}$ indices for BrS-S and BrS-A groups. The median [IQR] of each index and p-values segregated by BrS vs. control and BrS-S vs. BrS-A groups are shown in Table 2.

Table 2: Median[IQR] and p-value for $\text{TPEMR}_{\mathcal{O}}$, $\text{TPEMR}_{\mathcal{W}1}$ and $\text{TPEMR}_{\mathcal{W}2}$ at the different groups.

Group	$\text{TPEMR}_{\mathcal{O}}$	$\text{TPEMR}_{\mathcal{W}1}$	$\text{TPEMR}_{\mathcal{W}2}$
CG	0.006 [0.006]	0.005 [0.005]	0.002 [0.002]
BrS	0.009 [0.012]	0.007 [0.009]	0.004 [0.004]
p-value	0.014	0.009	0.010
BrS-S	0.011 [0.013]	0.008 [0.009]	0.004 [0.005]
BrS-A	0.008 [0.012]	0.006 [0.009]	0.003 [0.004]
p-value	0.130	0.130	0.024

4. Conclusions

T-wave peak-to-end morphology restitution index, TPEMR, shows significant differences between control and BrS patients, as well as between BrS-S and BrS-A patients when weighted warping is used. The small population of BrS-S may influence the statistical power of the results, so further studies with larger populations are required to evaluate the robustness of these findings.

Acknowledgments

Funding was provided by MICIN, Spain, projects: PID2022-140556OB-I00, CNS2023-143599 and TED2021-130459B-I00, and fellowship RYC2021-031413-I, and by Aragón Government group: BSICoS T39_23R.

References

[1] Antzelevitch C, et al. Brugada syndrome: report of the second consensus conference: endorsed by the heart rhythm society and the european heart rhythm association. Circulation 2005;111(5):659–670.

[2] Brugada J, et al. Present status of Brugada syndrome: Jacc state-of-the-art review. Journal of the American College of Cardiology 2018;72(9):1046–1059.

[3] Al-Khatib SM, et al. 2017 aha/acc/hrs guideline for management of patients with ventricular arrhythmias and the prevention of sudden cardiac death: a report of the american college of cardiology/american heart association task force on clinical practice guidelines and the heart rhythm society. Journal of the American College of Cardiology 2018; 72(14):e91–e220.

[4] Wilde AA, et al. The pathophysiological mechanism underlying Brugada syndrome: depolarization versus repolarization. Journal of Molecular and Cellular Cardiology 2010; 49(4):543–553.

[5] PAK HN, et al. Spatial dispersion of action potential duration restitution kinetics is associated with induction of ventricular tachycardia/fibrillation in humans. Journal of Cardiovascular Electrophysiology 2004;15(12):1357–1363.

[6] Ramírez J, et al. T-wave morphology restitution predicts sudden cardiac death in patients with chronic heart failure. Journal of the American Heart Association 2017; 6(5):e005310.

[7] Gómez N, et al. T-wave peak-to-end changes quantified by time-warping predicts ventricular fibrillation in a porcine myocardial infarction model. IEEE Transactions on Biomedical Engineering 2024;1–10.

[8] Martínez JP, et al. A wavelet-based ECG delineator: evaluation on standard databases. IEEE Transactions on Biomedical Engineering 2004;51(4):570–581.

[9] Gómez N, et al. Time-warping analysis of the T-wave peak-to-end interval to quantify ventricular repolarization dispersion during ischemia. IEEE Journal of Biomedical and Health Informatics 2023;1–12.

[10] Palmieri F, et al. Weighted time warping improves T-wave morphology markers clinical significance. IEEE Transactions on Biomedical Engineering 2022;69(9):2787–2796.

Address for correspondence:

Neurys Gómez Fonseca, Campus Río Ebro, I+D Building, D-5.01.1B, C. Mariano Esquillor, s/n, 50018 Zaragoza (Spain)
ngomez@unizar.es